Izvirni znanstveni članek

TEHNIKA -
računalniške tehnologije

ANALI PAZU
11/ 2021/ 1-2: 38-51

New generation impact and vibration insulation based on high pressure force-network technology

Nova generacija udarne in vibracijske izolacije na osnovi visokotlačne omrežne tehnologije

M. Bek[1], A. Aulova[1], A. Oseli[1] in I. Emri[1]

1 Center for Experimental Mechanics, Faculty of Mechanical Engineering, University of Ljubljana, Ljubljana, Slovenia

E-Mails: marko.bek@fs.uni-lj.si; alexandra.aulova@fs.uni-lj.si; alen.oseli@fs.uni-lj.si; ie@emri.si

* Avtor za korespondenco: I. Emri, ie@emri.si

Abstract: The article reviews the know-why and the know-how of an invention based on the patented dissipative granular high-pressure technology. It was found that by proper selection of damping material and hydrostatic pressure to which material is exposed during the loading, one can match material maximum damping properties with the frequency or rate of the applied loading. In this way one can fully utilize damping characteristics of the selected material and maximize the energy absorption properties of a damper. Using this unique potential of the dissipative granular high-pressure technology one can build ultimate damping elements that surpass the existing damping elements for sever orders of magnitude. Applications of such damping elements include for instance supports for industrial machines to damp vibrations, fundaments in building constructions to reduce susceptibility to earthquake damage and resonance, as well as trains and railway tracks to reduce vibration during travel, and to improve passive car safety in road transportation.

This article reviews phenomenological description of the time-dependent response of polymeric material when excited by impact- or vibrational loading needed in development of the new generation impact- and vibration isolation.

Key words: effect of pressure; viscoelasticity; dissipative granular materials; damping elements; thermoplastic polyurethane; earthquake and railway isolation; passive car safety.

Povzetek: Članek obravnava znanje izuma, ki temelji na patentirani disipativni zrnati visokotlačni tehnologiji. Ugotovljeno je bilo, da je z ustrezno izbiro dušilnega materiala in hidrostatičnim tlakom, ki mu je material izpostavljen med nakladanjem, mogoče ujemati največje lastnosti dušenja materiala s pogostostjo ali hitrostjo uporabljene obremenitve. Na ta način lahko v celoti izkoristimo lastnosti dušenja izbranega materiala in povečamo absorpcijske lastnosti lopute. Z uporabo tega edinstvenega potenciala disipativne zrnate visokotlačne tehnologije je mogoče zgraditi vrhunske dušilne elemente, ki za nekaj vrst presegajo obstoječe dušilne elemente. Uporaba takšnih blažilnih elementov vključuje na primer nosilce za industrijske stroje za dušenje vibracij, temelje v gradbenih konstrukcijah za zmanjšanje dovzetnosti za potresne poškodbe in resonanco, pa tudi vlake in železniške tire za zmanjšanje vibracij med potovanjem in za izboljšanje pasivne varnosti avtomobilov na cestah prevoz.

Ta članek obravnava fenomenološki opis časovno odvisnega odziva polimernega materiala, ko ga vzbudi udarna ali vibracijska obremenitev, potrebna pri razvoju nove generacije izolacije udarcev in vibracij.

Ključne besede: učinek tlaka; visokoelastičnost; disipativni zrnati materiali; dušilni elementi; termoplastični poliuretan; potresna in železniška izolacija; pasivna varnost avtomobilov.

1. Introduction

Isolation against harmonic excitations is well understood and elaborated, whereas dampers for impact and non-harmonic excitations, such as collision of vehicles, foundation for high speed trains, forging machines, and protection against earthquakes, is still subject of intensive research and development. The most promising damping solutions are still viscoelastic dampers, which drawback is that dampers with a given geometry, made from materials with sufficient damping properties, have insufficient stiffness and vice versa. Figure 1 shows a schematic comparison of stiffness and damping of cylindrical elements made from different known materials. As seen from the diagram stiffness of existing materials can differ more than 107 times, and their corresponding damping more than 108 times!

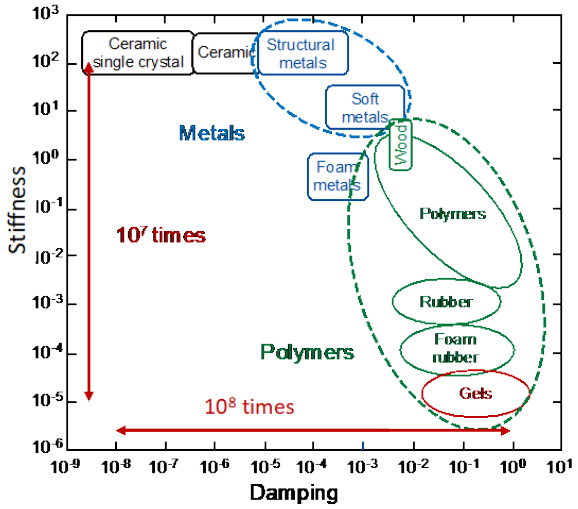

Figure 1: Comparison of damping and stiffness of a damper made from different known materials (adopted and modified from different sources)

These differences for typical engineering polymers that are used in damping applications are schematically shown in Fig. 2. In this case damping and stiffness may differ more than 1000 times.

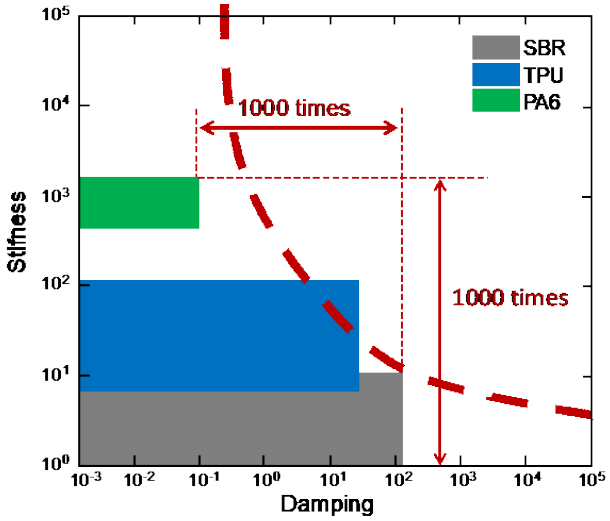

Figure 2: Comparison of damping and stiffness of a damper made from typical engineering polymers (adopted and modified from different sources).

From the two diagrams one may conclude that there is an engineering challenge how to overcome the shortcomings of the existing materials in order to construct dampers with required stiffness that will, at the same time, have desired energy absorption and damping properties. In different areas of application over the years many different engineering solutions have been developed which, however, still do not fulfil our expectations.

This rises the scientific question if it would be possible to increase stiffness of a selected material with desired damping and vice versa? The answer is positive!

In this paper we review the *know-why* and the know-how of an invention [1, 2] that is based on the so-called *dissipative granular high-pressure technology*. It was found that by proper selection of damping material and pressure to which material is exposed during the loading, one can match its maximum damping properties with the frequency or rate of the applied loading. In this way one would fully utilize damping characteristics of the selected material and maximize the energy absorption properties of the damper. Using this unique property of polymeric materials enabled us to design and build ultimate adaptive damping elements. For doing this one has to utilize a patented finding [1] that viscoelastic granular materials with properly selected multimodal size-distribution exhibit fluid-like behavior, while maintaining its behavior of the bulk material from which the granular material was made. Hence, such material may be used as a "pressurizing media" to impose inherent hydrostatic pressure on itself and consequently change its own damping properties.

The research-based invention utilizes knowledge that has been acquired over years in the field of characterization and mathematical modelling of time-dependent behavior of polymeric materials. We review and demonstrate that by utilizing the knowledge on the effect of inherent hydrostatic pressure on the time- and frequency-dependent behaviour of polymers it become possible to design and build the ultimate isolation against impact and non-harmonic excitations in different areas of application that surpasses existing isolations by several orders of magnitude.

In order to understand the know-why of the invention one needs to understand the fundamentals of time-dependent behaviour and its relation to thermo-mechanical boundary conditions to which material is exposed. More specifically, the interrelated effects of temperature and hydrostatic pressure on the material behaviour need to be investigated.

2. Theoretical background

Unlike elastic materials such as metals, ceramics, etc., polymers exhibit a so-called time-dependent behav-

ior, i.e, they undergo time-dependent changes in strain or stress under the application of external stress or strain. Figure 3 schematically presents comparison of material responses (strains) between elastic and viscoelastic materials under the application of a constant load (stress).

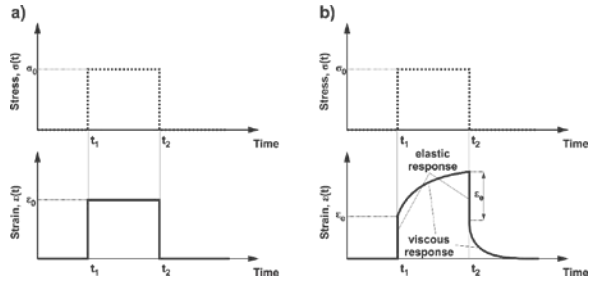

Figure 3: Responses (strains) of a) elastic and b) viscoelastic materials under the application of constant stress.

Due to the time-dependent nature of polymers, one can distinguish between two processes when material is subjected to an external load [3, 4]. These processes are creep and relaxation. They are distinguished by their type of external loading. In case of creep the applied loading is stress, and in case of relaxation the loading is strain. From a thermodynamic point of view, during relaxation material is »loaded« with a continously diminishing amount of energy. When all the imposed energy is consumed for molecular rearrangements, the relaxation process ceases. On the other hand, during creep, energy used for molecular rearrangement is continuously supplied to the material, and therefore a creep process effectively stops upon reaching the material equilibrium strain state, for crosslinked polymers, or failure of the material, for thermoplastic polymers.

Creep process

Creep process describes a time-dependent response of viscoelastic material in the form of a strain, ε(t), when it is subjected to a constant external load in the form of a stress, σ_0, commonly generated by a deadweight, [3, 4].

The general relationship for an uniaxial creep process is given as

$$\varepsilon(t) = \int_0^t D(t-u)\frac{d\sigma(u)}{du}du,$$

which, in the case when the applied stress has the form of a step function σ(u)=σ_0 h(u), simplifies into

$$\varepsilon(t) = \int_0^t D(t-u)\frac{d[\sigma_0 h(u)]}{du}du = \sigma_0\int_0^t D(t-u)\,\delta(u)du = \sigma_0 D(t),$$

where σ_0 is the magnitude of the applied stress, h(u) is the Heaviside function (step function), δ(u) is the Dirac function (impulse function), u is an integration variable of time, and D(t) is the time-dependent mechanical property of viscoelastic material called uniaxial creep compliance,

$$D(t) = \frac{\varepsilon(t)}{\sigma_0}.$$

Relaxation process

On the other hand, relaxation process describes a time-dependent response of viscoelastic material in the form of a decaying stress, σ(t), when it is subjected to the constant strain ε_0, [3, 4]. The general relationship for an uniaxial relaxation process is

$$\sigma(t) = \int_0^t E(t-u)\frac{d\varepsilon(u)}{du}du,$$

which, in the case when the applied strain has the form of a step function ε(u)=ε_0 h(u), simplifies into

$$\sigma(t) = \int_0^t E(t-u)\frac{d[\varepsilon_0 h(u)]}{du}du = \varepsilon_0\int_0^t E(t-u)\,\delta(u)du = \varepsilon_0 E(t),$$

where material function, E(t), called uniaxial relaxation modulus, has the form

$$E(t) = \frac{\sigma(t)}{\varepsilon_0}.$$

It is important to note that uniaxial creep compliance and relaxation modulus (or in general compliances and moduli) are not reciprocal values, i.e. E(t)≠1⁄D(t) , except for the limiting values, i.e., elastic instant values and equilibrium values. The two material response functions, creep-compliance and relaxation modulus, are related through a convolution integral interrelation,

$$\int_0^t E(t)D(t-u)du = t,$$

which is mathematically an inverse problem and requires special numerical techniques to be applied.

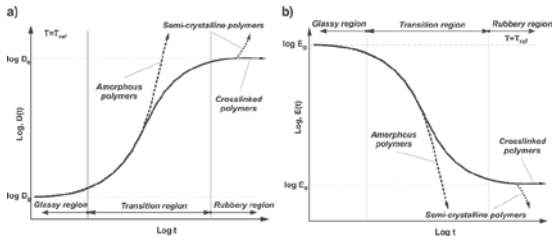

Figure 4: a) Creep and b) relaxation behavior for different types of polymers

Uniaxial creep and relaxation functions for different types of polymers are schematically shown in Fig. 4, where the index “g” and “e” denote the so-called *glassy* (elastic), and *equilibrium* value of the response respectively, which is typical for elastomers, thermosets and partially also for semi-crystalline polymers. Amorphous polymers do not have equilibrium values, since their molecular structure allow them to creep un-

til their mechanical failure or to relax until the process of the molecular rearrangement stops.

Material functions and constitutive description of time-depndent materials

Mechanical properties of time-dependent materials are also rate- and frequency-dependent, i.e., material response depends on the rate and frequency of the applied stress or strain. In general, viscoelastic behavior of solid polymer is determined with 21 material functions listed in Table 1 [3, 4]. They differ by type and mode of loading. Seven of them are obtained in the static mode and the remaining 14 in the dynamic mode of loading.

It is important to stress that Poisson's ration need to be determined from relaxation experiments and NOT from creep experiments, where deformations are changing with time.

Type of loading / Mode of loading			Uniaxial	Shear	Bulk (volumetric)	*Poisson's ratio*
Static	Relaxation		$E(t)$	$G(t)$	$K(t)$	$\vartheta(t)$
	Creep		$D(t)$	$J(t)$	$B(t)$	
Dynamic	Relaxation	In-phase	$E'(\omega)$	$G'(\omega)$	$K'(\omega)$	$\vartheta'(\omega)$
		Out-of-phase	$E''(\omega)$	$G''(\omega)$	$K''(\omega)$	$\vartheta''(\omega)$
	Creep	In-phase	$D'(\omega)$	$J'(\omega)$	$B'(\omega)$	
		Out-of-phase	$D''(\omega)$	$J''(\omega)$	$B''(\omega)$	

Table 1: Time-dependnt material functions

Within the framework of linear theory of viscoelasticity, material functions are interrelated in the Laplace space. Thus, it is sufficient to determine (measure) only two material functions in order to calculate the remaining 19 material functions [3]. Unfortunately, the interconversion procedures need to be done numerically. Table 2 presents the relations between material functions in the Laplace space, denoted with s.

Material function	Expressed as a function of					
	G and E	**G and ϑ**	**E and ϑ**	**K and E**	**K and ϑ**	**K and G**
K	$\frac{G(s)E(s)}{9G(s)-3E(s)}$	$\frac{2G(s)(1+\vartheta(s))}{3(1-2\vartheta(s))}$	$\frac{E(s)}{3(1-2\vartheta(s))}$	-	-	-
G	-	-	$\frac{E(s)}{2(1+\vartheta(s))}$	$\frac{3K(s)E(s)}{9K(s)-E(s)}$	$\frac{3K(s)(1-2\vartheta(s))}{2(1+\vartheta(s))}$	-
E	-	$2G(s)(1+\vartheta(s))$	-	-	$3K(s)(1-2\vartheta(s))$	$\frac{9K(s)G(s)}{3K(s)+G(s)}$
ϑ	$\frac{E(s)}{2G(s)}-1$	-	-	$\frac{1}{2}-\frac{E(s)}{6K(s)}$	-	$\frac{3K(s)-2G(s)}{6K(s)+2G(s)}$

	J and D	**J and ϑ**	**D and ϑ**	**B and D**	**B and ϑ**	**B and J**
B	$\frac{9D(s)}{-3J(s)}$	$\frac{3J(s)(1-2\vartheta(s))}{2(1+\vartheta(s))}$	$\frac{3D(s)(1-2\vartheta(s))}{}$	-	-	-
J	-	-	$2D(s)(1+\vartheta(s))$	$\frac{3D(s)}{-\frac{B(s)}{3}}$	$\frac{3B(s)(1+2\vartheta(s))}{3(1-2\vartheta(s))}$	-
D	-	$\frac{J(s)}{2(1+\vartheta(s))}$	-	-	$\frac{B(s)}{3(1-2\vartheta(s))}$	$\frac{B(s)}{9}-\frac{J(s)}{3}$
ϑ	$\frac{J(s)}{2D(s)}-1$	-	-	$\frac{1}{2}-\frac{B(s)}{6D(s)}$	-	$\frac{3J(s)-2B(s)}{6J(s)+2B(s)}$

Table 2: Relations between material functions in Laplace space

From the theory of elasticity it is known that shear and bulk material functions provide complete description for the material since stress-strain fields for solids in general, i.e. σ_{ij} and ε_{ij}, can be expressed through the sum of a deviatoric part which refers to changes of shape of a metarial, and a dilatometric part which refers to its changes in volume. The same is true for time-dependent behavior, however, their behavior should be presented in an integral formulation,

$$\sigma_{ij}(t) = 2\int_0^t G(t-u)\frac{d\varepsilon_{ij}(u)}{du}du + \delta_{ij}\int_0^t K(t-u)\frac{d\varepsilon_{kk}(u)}{du}du, \quad \text{and}$$

$$\varepsilon_{ij}(t) = \frac{1}{2}\int_0^t J(t-u)\frac{d\sigma_{ij}(u)}{du}du + \frac{1}{3}\delta_{ij}\int_0^t B(t-u)\frac{d\sigma_{kk}(u)}{du}du,$$

where *u* represents an integral variable of time, *G(t)* and *K(t)* are shear and bulk relaxation moduli, and *J(t)* and *B(t)* are shear and bulk creep compliances, respectively. Since time-dependent changes in bulk properties are small (changes in time are from 2 to 4 times) in comparison to time-dependent changes in shear properties, which can change in time for orders of magnitude (from 100 to 10000 times) [3-7]. Therefore, for many engineering applications one may consider that the time- or frequency/rate-dependent behavior of polymers and products made from polymeric materials, are primarily governed by shear material functions. Therefore, shear material functions will be used to explain the effect of temperature and the effect of pressure on the mechanical behavior of polymers.

2.1. Effect of temperature

The effect of temperature on the time-dependent behavior of polymers may be described by a so-called free volume concept. This concept is stating that behavior of polymers, regardless of the type or mode of loading, is solely governed by the rate of molecular rearrangements accuring inside the material, whereas the rate depends on the instantly available free volume to allow the rearrangements of the polymer chains.

By increasing the temperature, segmental mobility or molecular rearrangements in a polymer increases [5-7]. This so called micro-Brownian thermal motion causes and increase the free volume, i.e., an increas of available space for relative motion of molecules under the application of loading, and thereby accelerates creep or relaxation processes. On a macroscale, this phenomenon can be observed as horizontal shift of time-dependent mechanical properties to shorter times along the logarithmic time-axis, as schematically shown in Fig. 5 for the case of crosslinked materi-

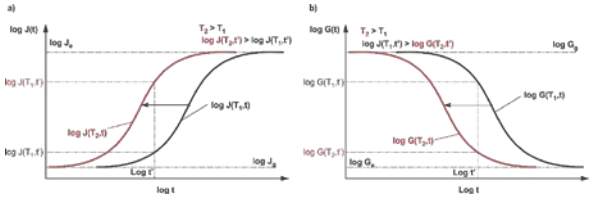

Figure 5: Effect of temperature on a) shear creep compliance and b) shear relaxation modulus

als. In both cases, for shear creep compliance, Fig. 5a, and for shear relaxation modulus, Fig. 5b, an increas of temperature from T_1 to T_2 will cause a parallel shift of the response function towards shorter times.

From Fig. 5 one observes that material property at a given time strongly depends on material temperature. Teherefore, one cannot talk about time-dependent behavior of polymeric materials without stating the temperature at which this behavior was observed!

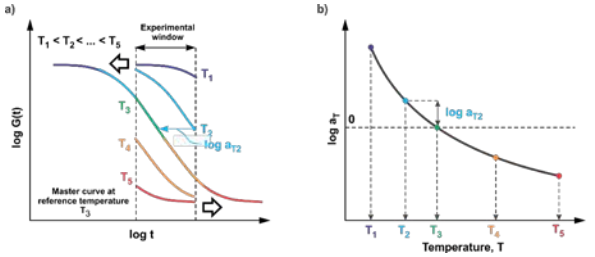

Figure 6: a) generation of master curve at $T_{ref}=T_3$ for a case of shear relaxation modulus and b) representation of shift factors as function of temperature

Figure 6a shows curve segments of the mechanical behavior measured at different temperatures T_1 through T_5, and the master-curve for the reference temperature T_3 obtained from horizontal shifting. Figure 6b shows the corresponding shift factors as function of temperature. The function log a_T (T) is often called the thermal shift-function. According to the existing knowledge, the time-temperature superposition may be applied for thermorheological simple materials. These are primarily single-phase or single transition homopolymers and random copolymers. Thermorheological simplicity requires that all respondance times, i.e. relaxation and retardation times depend equally on temperature for which one can express thermal shift-functions [6], as

$$a_T(T) = \frac{t_i(T)}{t_i(T_0)}, \quad i = 1, 2, 3, \ldots$$

or in logarithmic scale,

$$\log a_T(T) = \log t_i(T) - \log t_i(T_0), \quad i = 1, 2, 3, \ldots$$

There are many theories used for modeling the effect of temperature on the time-dependent behavior of polymers [6], however the most well known model was proposed by Williams, Landel and Ferry in 1955 [8], known as the WLF model,

$$\log a_T(T) = -\frac{(B/2{,}303 f_0)(T - T_0)}{f_0/\alpha_f + T - T_0} = -\frac{c_1^0(T - T_0)}{c_2^0 + T - T_0} = -\frac{c_1^0 \Delta T}{c_2^0 + \Delta T}$$

where c_1^0, c_2^0, and B are material constants, and f_0 and α_f are the fractional free volume and the corresponding volumetric thermal expansion coefficient, respectively, all determined at the reference temperature T_0.

The shifting is the »weakest step« of time/temperature–, and time/pressure– (discussed in continuation) superposition procedure. In the past shifting was performed »manually«. Recently this problem has been resolved by our team [10]. We have developed the closed form mathematical methodology for performing the time-temperature and/or time-pressure superposition, called CFS-algorithm, which completely removes issues related to »manual« shifting procedure. CFS methodology recently became the new ISO 18437-6:2017 standard .

The proposed mathematical formulation of the shifting procedure takes into account that material functions measured at two different temperatures represent the material behavior at two different thermodynamic states, which differ in the corresponding Gibbs free energy [11] by

$$\Delta W = \int_{T_0}^{T_k} S dT,$$

where W denotes Gibbs free energy, S is the internal entropy of the material, while T_0 and T_k represent two selected equilibrium thermodynamic states at which the corresponding segments of the material function have been measured. The rate at which mechanical energy is absorbed per unit volume of a viscoelastic material at a given boundary condition T_k is equal to the *stress power*, i.e. the rate at which work is performed. The stress power at time t is defined as

$$dW(t, T_k)dt = \sigma(t, T_k)\frac{d\varepsilon(t)}{dt}.$$

The absorbed mechanical energy causes material inherent structural (molecular) rearrangements during the relaxation or creep process. Thus, any two segments of the material function, measured at the reference state T_0, and any other selected state T_k, that need to be superimposed (shifted) into a master curve should have the same energy release rate at all points of the superimposing interval. This criterion may be expressed as

$$\left.\frac{dW(t, T_o)}{d\log t}\right|_{t=t_j} = \left.\frac{dW(t, T_k)}{d\log t}\right|_{t=t_k}.$$

Equation (15) is fulfilled when the overlapping area H between two segments is equal to zero, as shown in Fig. 7.

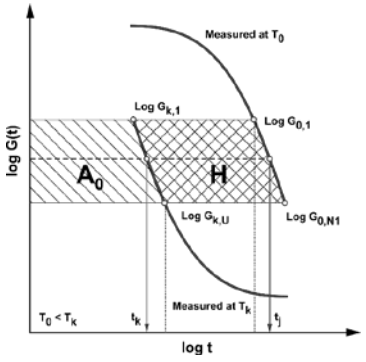

Figure 7: Schematics of the CFS procedure for an example of shear relaxation modulus

This yields to the closed form equation for the shift factor

$$\log a_{T_k} = \frac{\sum_{i=1}^{U-1}\left[\frac{\log t_{k,i+1}+\log t_{k,i}}{2}\cdot\left(\log G_{k,i+1}-\log G_{k,i}\right)\right]-A_0}{\log G_{0,N_1}-\log G_{0,1}},$$

where

$$A_0 = \sum_{i=1}^{N_1-1}\frac{\log t_{0,i}+\log t_{0,i+1}}{2}\cdot\left(\log G_{0,i+1}-\log G_{0,i}\right).$$

For further details, see Gergesova et al. [10] and the new ISO 18437-6:2017 standard.

2.2 Effect of pressure

Hydrostatic pressure can be presented as a stress loading, since pressure is essentially a 3D stress, i.e., $p=\sigma_{kk}$. Pressure affects polymers in the solid state as well as in the molten state. When a polymeric material is pressurized, and simultaneously exposed to an external mechanical excitation of strain or stress, not only the local movement of molecules is constrained, but also their relative motion to each other is hindered. Consequently, molecular rearrangements enforced by external loading are slowed down, which on the macroscale is observed as a slow-down in the creep and relaxation processes. Hence, hydrostatic pressure causes changes in the macroscopic time-dependency of polymers. The effect of pressure on creep and relaxation process is demonstrated in Fig 8. As shown, higher pressure, $p_2>p_1$, shifts the material properties to longer times, which indicates that the applied pressure affects all molecular processes equally. Hence, increased pressure does not change the shape of the response functions but moves them in parallel along the logarithmic time-axis.

Suppose that the shaded areas in Fig 8 indicate a material lifetime. Considering that pressure shifts creep and relaxation response functions to longer times one may conclude that by exposing material to high enough pressure its glassy state properties may extend the lifetime of a product.

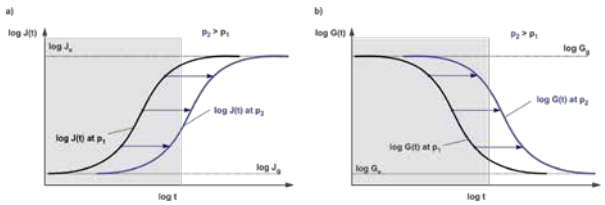

Figure 8: Shift of the creep compliance (left) and relaxation modulus (right) towards longer times under applied pressure. Schematics presents behavior of crosslinked elastomers.

On the macro scale an increase of pressure to which material is exposed has similar effect on material mechanical properties as a decrease in temperature. In both cases we observe "shifting" of response functions along the logarithmic time scale. Hence, similar to the time-temperature superposition, we may talk about the time-pressure superposition principle. However, they are governed by different processes on the molecular scale. A temperature change causes a change in the average kinetic energy of polymeric molecules, while a change in pressure does not change the energy state of the molecules but limits the available space for local molecular movements.

Time-pressure superposition

The time-pressure superposition principle allows shifting of response function segments, measured at different isobaric conditions, into a single "master-curve" that extends over a time scale beyond what can be normally measured in a real-time experiment at reference room conditions. It has to be stressed that time-pressure superposition principle may be applied only for piezo-rheologically simple materials. These are materials where all molecular groups equally respond to the applied pressure. Time-pressure superposition is (still) not sufficiently investigated, therefore it is not clear if it is walid for multi-phase materials, such as block- and graft- copolymers, hybrid materials, polymers blends, and bituminous materials [4-6].

On the macro scale, the time-pressure superposition works similarly as the time-temperature superposition. Experiments are performed at different pressures while maintaining the temperature constant. Measured segments of relatively short times at different pressures allow construction of the so-called master-curve, which defines behavior of a material at selected reference pressure and temperature conditions, as shown in Figure 9a. For each particular segment the amount of shifting required to construct the mastercurve is specified with the shift factor a_pi. The sign of the shift factor for a particular pressure p_i is determined by the shift direction of the segment relative to the reference pressure ($p_i=p_{ref}$) at which the mastercurve is constructed. Shift factors corresponding to higher pressures (relative to the reference pressure) are positive, since they move the mastercurve to longer times. In addition, one obtains the interrelation between the applied pressure and the corresponding shift factors, as demonstrated in figure 9b.

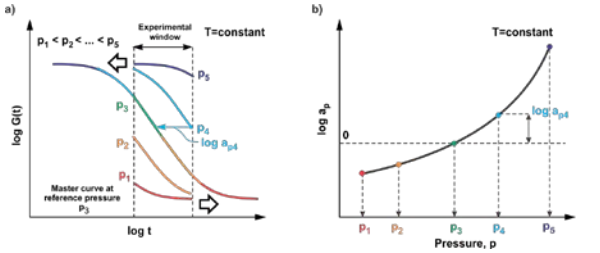

Figure 9: a) Segments of shear relaxation modulus measured at different pressures and the mastercurve composed by shifting the segments for the reference pressure p_3; b) shift factors a_p in dependence on pressure

Shifting of the measured segments should be pereformed with the standardized CFS algorithm (ISO 18437-6:2017) proposed by Gergesova et al. [10].

Modelling the effect of pressure on polymers

Over years, several models were developed that are capable of accounting for the pressure effect on mechanical properties of polymers. Among those most universal models are the FMT model, proposed by Fillers, Moonan and Tschoegl [12], and the Knauss-Emri model [13], where both models consider simultaneous effects of temperature and pressure. The FMT model is applicable for describing the effect of pressure and temperature in the equilibrium state, while the Knauss-Emri model may be used for modeling material behavior under varying temperature and pressure conditions, i.e., under conditions when material is not in its thermodynamic equilibrium. It is important to mention that when pressure and temperature are constant the Knauss-Emri model reduces to the WLF and FMT equations.

Since impact loading is time-varying loading, the appropriate model is the Knauss-Emri model [13], where the stress-strain relations are expressed through deviatoric part, $S_{ij}(t)$, which refers to changes of shape, and a dilatometric part, $\sigma_{kk}(t)$, which refers to changes in volume,

$$\sigma_{kk}(t) = 3\int_0^t K[t'(t) - \xi'(\xi)]\frac{\partial\theta(\xi)}{\partial\xi}d\xi,$$

$$S_{ij}(t) = 2\int_0^t G[t'(t) - \xi'(\xi)]\frac{\partial e_{ij}(\xi)}{\partial\xi}d\xi,$$

where

$$t'(t) - \xi'(\xi) = \int_\xi^t \frac{du}{\phi[T(u),\theta(u)]},$$

$$\log\phi[T(u),\theta(u)] = \frac{b}{2.303}\left[\frac{1}{f[T(u),\theta(u)]} - \frac{1}{f_0}\right], \text{and}$$

$$f[T(u),\theta(u)] = f_0 + \int_0^u \alpha(u-\lambda)\frac{\partial T(\lambda)}{\partial\lambda}d\lambda + \frac{1}{3}\int_0^u B(u-\lambda)\frac{\partial\sigma_{kk}(\lambda)}{\partial\lambda}d\lambda.$$

Here *K(t)* and *G(t)* are time-dependent bulk- and shear- modulus, and B(t)=*K*^(-1) (t) is the time-dependent bulk creep compliance (an inverse of time-dependent bulk modulus), *f*_0, and *α*_f (t) are the fractional free volume and the corresponding time-dependent volumetric thermal expansion coefficient, all determined at reference temperature, *T*_0, and pressure *p*_0. To measure the required above mentioned material functions one needs a special measuring system that was developed and elaborated by our group and it is briefly presented in continuation.

Characterization of the effect of pressure on polymers

To measure the material functions needed in the Knauss-Emri model, an unique experimental setup was developed by Moonan and Tschoegl [12] , which was later upgraded by Kralj, Prodan and Emri [14, 15].

The measuring system is schematically presented in Fig. 10, and consist of four subsystems. The first is the *thermal subsystem*, consisting of a circulator and thermal bath that allows measurements to be performed at different temperatures. The second is the *pressurizing subsystem*, consisting of a pressure vessel, piping and a hand pump that allow measurements to be performed at different pressures. The third is the *electronic subsystem*, consisting of an electromagnet, permanent magnet and motor charger, carrier amplifier and data acquisition, used for controlling specimen excitations and signal acquiring, data storing and their analysis. The fourth is the *measuring subsystem*, consisting of two measuring inserts: relaxometer and dilatometer, shown in Fig. 11. The measuring system allows measurements of thermo-mechanical time-dependent properties of polymers at different temperature and pressure conditions, ranging from -50°C to 120°C and 0.1 to 500 MPa, respectively.

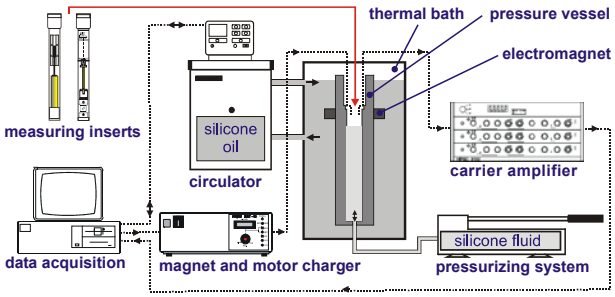

Figure 10: Schematic representation of the measuring system

The relaxometer, Fig. 11a, is used for measuring time-dependent mechanical properties in shear. The specimen is subjected to a load in a form of a constant torsional angle or shear strain, applied by the loading device, consisting of a triggering mechanism and electric motor. By measuring the torque moment via a load cell, one can measure the decaying shear stress. Knowing the applied cause (i.e., the constant shear strain), and the resulting response (i.e., decaying shear stress) of the material, one can determine the time-dependent shear relaxation modulus at different temperature and pressure conditions.

The dilatometer, Fig. 11b, is used to measure time-dependent bulk (volumetric) properties of polymers at different temperature and pressure conditions. Measurements are performed by monitoring changes in the length of the specimen L(t,T,p), which result from the imposed changes in pressure and/or temperature using a built-in Linear Variable Differential Transformer (LVDT). For isotropic materials the volume V(t,T,p) can be estimated from the relative change in length, by assuming that relative change of specimen dimensions is equal in all direction. Knowing the volume change

of a specimen one can determine different thermo-mechanical properties of polymers, such as the bulk creep compliance $B(t,T,p)$, equilibrium bulk creep compliance $B(T,p)=B(t\to\infty,T,p)$, equilibrium bulk modulus, $K(T,p)=K(t\to\infty,T,p)=1/(B(t,p))$, linear thermal expansion coefficient $\alpha(T,p)=\alpha(t\to\infty,T,p)$, volumetric thermal expansion coefficient $3\alpha(T,p)=3\alpha(t\to\infty,T,p)$, and compressibility $\beta(T,p)=\beta(t\to\infty,T,p)$.

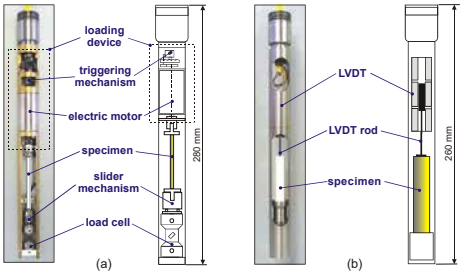

Figure 11: (a) relaxometer insert and (b) dilatometer insert of the measuring system

As an example, we show experimental results on shear relaxation modulus for semicrystalline polyamide 6 (PA6), Fig. 12, and elastomeric natural rubber, Fig. 13. Both materials are commonly used for damping vibrations and impact loading. The diagrams on the left show measured segments at indicated constant pressures, whereas the diagrams on the right show the corresponding master curves.

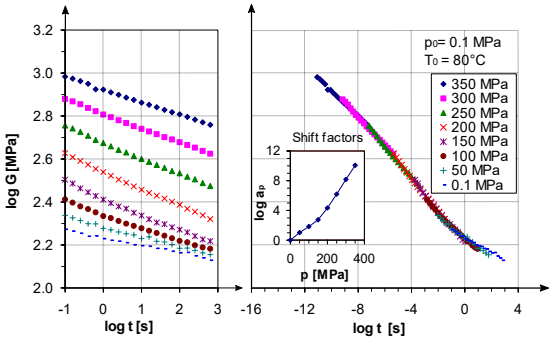

Figure 12: Polyamide 6 PA6: a) shear relaxation modulus segments measured at different pressures and b) segments shifted to mastercurve with the shift factors

Figure 12 displays behavior of PA6. Even though PA6 is a semicrystalline material, the range of pressures available for measurements of shear relaxation modulus at selected reference temperature was not high enough to reach the material glassy state. Therefore, in Fig. 12, only the transition region of the shear modulus is visible.

Natural rubber is a cross-linked material, which means that it should exhibit both glassy and equilibrium plateaus. However, at the highest pressure of 400 MPa material starts to enter its glassy plateau, whereas at atmospheric pressure it again only starts to approach its rubbery equilibrium plateau, Fig. 13. To reach both plateaus one would need to perform experiments at higher temperatures and much higher pressures.

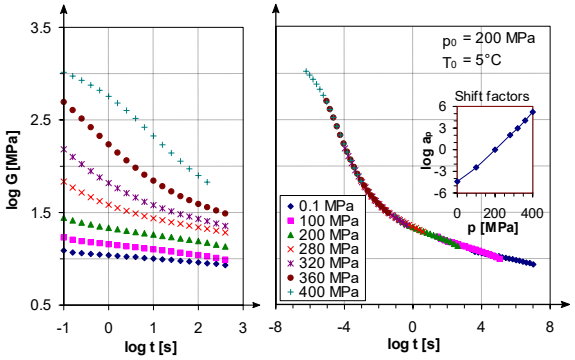

Figure 13: Natural rubber, NR: a) shear relaxation modulus segments measured at different pressures and b) segments shifted to mastercurve with the shift factors

Natural rubber is a cross-linked material, which means that it should exhibit both glassy and equilibrium plateaus. However, at the highest pressure of 400 MPa material starts to enter its glassy plateau, whereas at atmospheric pressure it again only starts to approach its rubbery equilibrium plateau, Fig. 13. To reach both plateaus one would need to perform experiments at higher temperatures and much higher pressures.

3. Flowability of granular systems

We found [1, 2] that viscoelastic granular materials with properly selected multimodal size-distribution exhibit fluid-like behavior, while maintaining behavior of the bulk material from which they were made. Hence, they may be used as "pressurizing media" to impose inherent hydrostatic pressure on itself within a flexible rigid container, and consequently change its own damping properties. In order to obtain a hydrostatic pressure within the granular system one need to be able to measure flowability (readiness to flow) of a granular material in the state of no-motion, i.e., the so-called zero-rate fluidity. In order to study the so-called zero-rate fluidity of granular systems we have developed a new apparatus, called the Granular Friction Analyzer (GFA) [16-18].

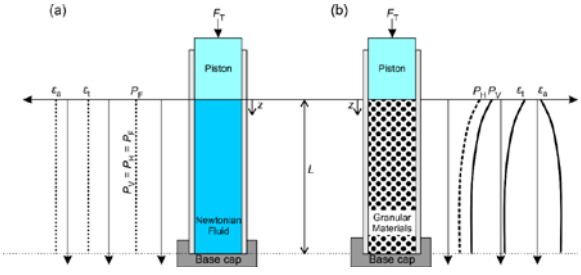

Figure 14: Schematics of vertical PV(z) and horizontal PH(z) internal pressure; and axial εa (z) and tangential εt (z) strains at uniaxial compression in the case of (a) Newtonian fluid and (b) Granular material

The design of the GFA apparatus is based on the realization that Newtonian fluids have unique property to redirect forces applied to them to all directions equally, and throughout the volume they occu-

py. Hence, if we expose a Newtonian fluid to uniaxial compression loading F_T within a closed cylinder, via a piston, the pressure distribution in all directions will be constant, $p_F=F_T/A=p_V=p_H$, as shown in Fig. 14a. On the other hand, if we expose granular material to the same load, the pressure distribution in axial z-direction will diminish with the distance from the piston, as shown in Fig. 14b. Since one cannot measure pressure distribution directly, one should measure deformation of the cylinder surface in axial, ε_a (z), and tangential, ε_t (z), direction along the axis of the cylinder, using straingauges [17], or digital immage correlation (DIC) technic [18].

As a measure of the flowability of granular materials we have introduced the GFA index for characterizing the flow behaviour of granular materials under uniaxial compression loading. The calculation of the GFA index is based on the integration of the internal pressure distribution along the cylinder wall, within which the granular material is being uniaxially compressed by a piston, and normalized by the pressure distribution of a Newtonian fluid [17, 18],

$$GFA_{\text{index}} = \frac{\int_0^L P_V(z)dz}{P_F.L} = \frac{A}{F_T.L}\int_0^L P_V(z)\,dz,$$

where

$$P_V = \frac{4.F_V}{\pi D_i^2.(1+\varepsilon_t)^2},$$

$$F_V = F_T + \pi D_i.(1+\varepsilon_t).t_w.\sigma_a,$$

and

$$\sigma_a = \frac{E_w(\varepsilon_a + \nu_w.\varepsilon_t)}{1-\nu_w^2}$$

Here D_i is the inner diameter of the cylinder, whereas E_w, ν_w, ε_t and ε_a denote the Young's modulus, the Poisson's ratio, and the tangential and axial strain of the cylinder wall, respectively. Taking the measurements of tangential $\varepsilon_{\_t}$ and axial strain ε_a on the cylinder wall in *n* points along the z axis the related vertical internal pressure P_V (z) can be calculated and based on that the GFA-index.

We have used the GFA apparatus and the GFA-index to optimize the flowability of granular materials used in the new generation damping elements. Granular materials with properly selected flowability may be used as "pressurizing media" to impose inherent hydrostatic pressure on itself within a flexible rigid container, and, consequently, change its own stiffness and damping properties.

4. Advanced impact and vibration isolation

The existing solutions for structural and vibration control do not and cannot fully utilize damping characteristics of time- and frequency-dependent materials because their maximal damping properties are located at frequencies that are far away from the frequency range of engineering interest, as it is schematically shown in Fig. 15.

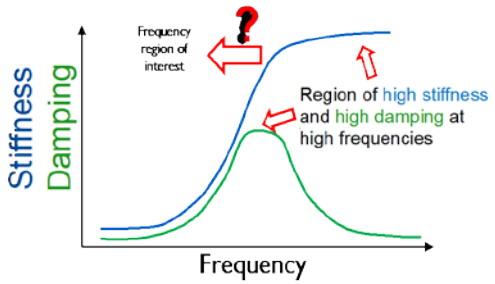

Figure 15: Frequency dependence of damping for materials used in vibration and impact isolations

The frequency domain material functions may be obtained through the interconversion from the corresponding creep and relaxation functions measured in time domain [3, 9],

$$G'(\omega) = \omega\int_0^\infty G(t)\sin\omega t\,dt, \quad G''(\omega) = \omega\int_0^\infty G(t)\cos\omega t\,dt$$

and

$$J'(\omega) = \omega\int_0^\infty J(t)\sin\omega t\,dt, \quad J''(\omega) = \omega\int_0^\infty J(t)\cos\omega t\,dt,$$

where G'(ω) and J'(ω) are the storrage modulus and storrage complaince, and G''(ω) and J''(ω) are the loss modulus and loss compliance, respectively. The first two represent material stiffness, whereas the last two its damping and energy absorption properties.

As it was shown, by exposing material to hydrostatic pressure their properties will be shifted along the logarithmic time- and frequency-scale. In time-domain increased pressure shifts material properties to longer times, while in frequency-domain all four material functions, the storrage modulus and storrage complaince, and the loss modulus and loss compliance are shifted to the left towards lower frequencies, as it is shematically shown with the arrow in Fig. 15. Hence, by proper selection of a hydrostatic pressure to which material is exposed one can match the frequency range of its maximum damping properties with the resonance frequency of the selected vibrating structure, or with a rate of an impact loading. In this way we can fully utilize damping characteristics of the selected damping material and maximize the energy absorption properties of a damper.

Now, an immediate question is how to generate the hydrostatic pressure within a selected damping material? The easiest engineering solution would be to use a uniaxial or bi-axial loading. Unfortunately, this is not possible! Pressure is a sum of principle stresses, $p=\sigma_{11}+\sigma_{22}+\sigma_{33}$, and as soon as the applied loading

is not three dimensional the shear stresses will appear and, before reaching the pressures that are needed to shift material functions, the shear stresses will reach a critical value and damping material will fail. This is schematically demonstrated in Fig. 16.

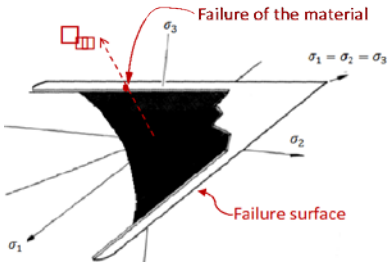

Figure 16: Material failure envelope

As mentioned in section 3, the inventive solution is to use granular materials for which it is valid that as dimension of particles becomes smaller the shear stresses within the material diminish faster than the principle stresses,

$$\lim_{V \to 0} \frac{\sigma_{kk}}{S_{ij}} = \infty \ .$$

At the same time, as flowability analysis showed, granular materials when excited beyond a certain level of stress flow similarly as liquids while maintaining all properties of a bulk material. Hence, micro- to macro- size multimodal elastomeric granular material may be used as a pressurizing media (similarly as air in tires) to impose hydrostatic pressure on themselves, and change frequency dependence of its own energy absorption properties. With proper adjustment of pressure, we also adjust the stiffness of the damping element (again, similar as with air in tires). Our proposed solution consists of micro- and macro-sized particles [1,2]. Smaller particles lead to more surface area per unit volume, which increases the magnitude of frictional dissipation energy caused by particle-particle interaction; while larger particles will allow macroscopic flow, as described above. Hence, our proposed solution utilizes all possible energy dissipation mechanisms and represents an optimal (ultimate) solution for the proposed novel damping system. Such patented damping elements [1, 2] consist of elastomeric granular material, which is encapsulated in a flexible tube made out of rigid fibers, as schematically shown in Fig. 17.

This design enables us to pressurize the granular material inside the damping element. At higher pressures properties of material shift to lower frequencies, compared to the reference values, see Fig. 18.

Working principle of such damping element is schematically explained in Fig. 18. The bell-shaped solid line shows the "original" dynamic response of a structure exposed to, for example, an earthquake excitation and, as a dashed line, the reduced dynamic response of the structure when the new damping elements are applied. The solid line on the right-hand side of Fig. 18 schematically shows the energy absorption frequency dependence of an elastomeric granular material at atmospheric pressure p_0. If the same elastomeric material is pressurized to a properly selected pressure $p>p_0$ its damping properties may be frequency adjusted such so to match the earthquake excitation frequency, shown with the dashed line, and reduce the dynamic response of the structure

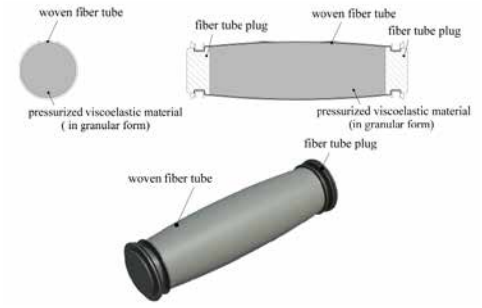

Figure 17: Damping elements consisting of pressurized elastomeric granular material within a tube made from rigid fibers.

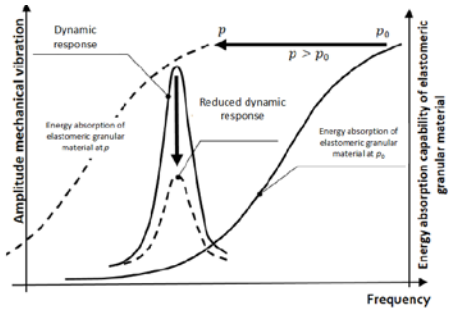

Figure 17: Damping elements consisting of pressurized elastomeric granular material within a tube made from rigid fibers.

Experimental results on TPU

As an example, we show the results of the effect of hydrostatic pressure on stiffness and damping properties of a commercial TPU material from the Elastollan® 11 series , i.e., 1190A, which is already used in manufacturing of vibration insulation.

Material stiffness is represented with the storage modulus $G'(\omega)$, whereas its damping by the loss modulus $G''(\omega)$. The experiments to determine TPU's $G'(\omega)$ and $G''(\omega)$ pressure dependence were performed on our high-pressure experimental setup presented above. For details on experimental procedure see [19].

For clarity reasons the results on storage $G'(\omega)$, and loss modulus $G''(\omega)$ are shown for only two pressures, i.e., 1 bar and 2000 bar. The full symbols present measurements done at lower pressure, p=1 bar, whereas the empty symbols present measurements done at higher pressure, p=2000 bar. The results for the stor-

age modulus $G'(\omega)$ are shown in Fig. 19, and for the loss modulus $G''(\omega)$ in Fig. 20. As expected, the value of both material functions representing stiffness and damping greatly increase as the pressure is increased from 1 to 2000 bar.

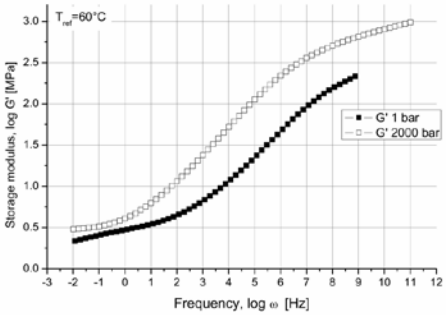

Figure 19: Storage modulus, $G'\omega$), at p=1 bar and p=2000 bar

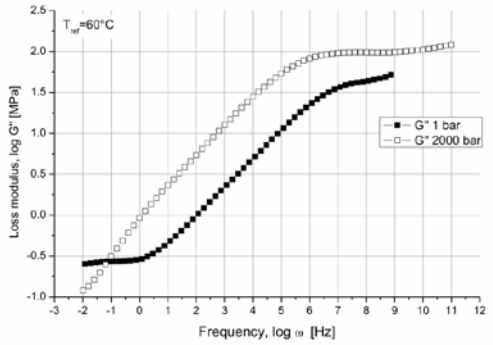

Figure 20: Loss modulus $G''(\omega)$ at ***p*=1 bar and p=2000 bar**

Since the vibrations and noise causing the most discomfort are located in the frequency range between 1 and 1000 Hz, we will examine the effect of hydrostatic pressure on TPU material stiffness, represented by G'(ω), and TPU material damping, represented by G''(ω), at 1 Hz and 1000 Hz, at a reference temperature T_{ref}=60°C. Comparison is shown in Fig. 21.

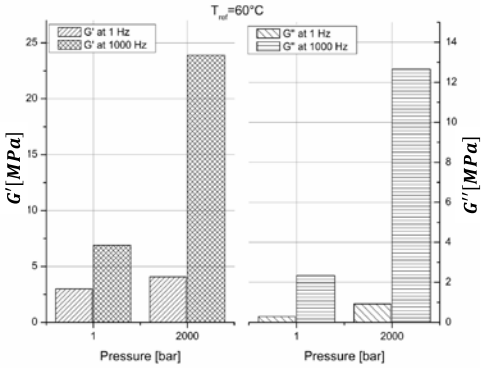

Figure 21: Storage, **G'(ω)**, and loss, **G''(ω)**, modulus of TPU at **p=1 bar** and **p=2000 bar** at 1 HZ and 1000 Hz.

Figure 21 contains two diagrams, the left diagram shows the effect of pressure on G' (ω), and the right diagram the effect of pressure on G'' (ω). In both cases is shown material performance at 1Hz and 1000Hz. At frequency 1 Hz and pressure 1 bar, the storage modulus is G' (ω=1Hz,p=1bar)=2.99MPa, whereas at pressure 2000 bar the storage modulus increases to G' (ω=1Hz,p=2000bar)=4.07MPa. Hence, material becomes 1.4 times stiffer. At the same frequency of 1Hz the loss modulus at pressure 1 bar is G'' (ω=1Hz,p=1bar)=0,29MPa, whereas at pressure 2000 bar it rises to G'' (ω=1Hz,p=2000bar)=0,92MPa. This means that at elevated pressure the materials ability to dissipate energy increases 3.15 times.

At ω=1000 Hz, we observe analogous trends. At 1bar the storage modulus is G' (ω=1000Hz,p=1bar)=6.899MPa, whereas at the pressure 2000 bar the storage modulus becomes G' (ω=1000Hz,p=2000bar)=23.89MPa, meaning that material stiffness is increased 3.46 times. At the same time the loss modulus at pressure 1 bar isG'' (ω=1000Hz,p=1bar)=2.33MPa, and at pressure 2000 bar it becomes G'' (ω=1000Hz,p=2000bar)=12.65MPa. Thus, the material ability to dissipate energy has increased 5.41 times.

Of course, by further increasing material hydrostatic pressure one may increase the stiffness and damping properties much further, as it is demonstrated in continuation.

Stiffness of an isolation depends on its geometry and the storage modulus of a material from which it is built, whereas, its energy absorption capability is defined by isolation total volume and material loss modulus. Hence, if we keep the geometry and volume of an isolation constant both its stiffness and its energy absorption capability will depend on material storage and loss modulus only. In fact, the main interest is to understand how much (how many times) we can increase stiffness and energy absorption of an isolation by exposing the material from which it is made of to a selected hydrostatic pressure. Therefore, we introduce two coefficients, first, defining the increase of isolation stiffness by exposing it to a selected hydrostatic pressure p, relative to the isolation stiffness at the environmental pressure p0 = 0.1MPa:

$$K_k(p,\omega) = \frac{G'(p,\omega)}{G'(p_0,\omega)} .$$

and the second

$$K_d(p,\omega) = \frac{G''(p,\omega)}{G''(p_0,\omega)} .$$

which defines an increase of isolation energy absorption (damping) obtained by exposing the analyzed TPU to a selected hydrostatic pressure. Comparison is made within the frequency range (1 - 10000Hz), which is of main interest for an impact and vibration isolation. The results are shown in two different forms: (i) $K_k(p,\omega)$ and $K_d(p,\omega)$ as functions of frequency, for four different pressures; and (ii) $K_k(p,\omega)$ and $K_d(p,\omega)$ as functions of hydrostatic pressure, for four different

frequencies. In fact, all mentioned diagrams present the same information, i.e., how much hydrostatic pressure we need at a given frequency to obtain a selected increase of isolation stiffness and energy absorption.

Figure 22 shows $K_k(p,\omega)$ and $K_d(p,\omega)$ at four selected pressure conditions, i.e., , 50, 100, 200 and 300 MPa, as functions of frequency within the frequency range 1-10000Hz.

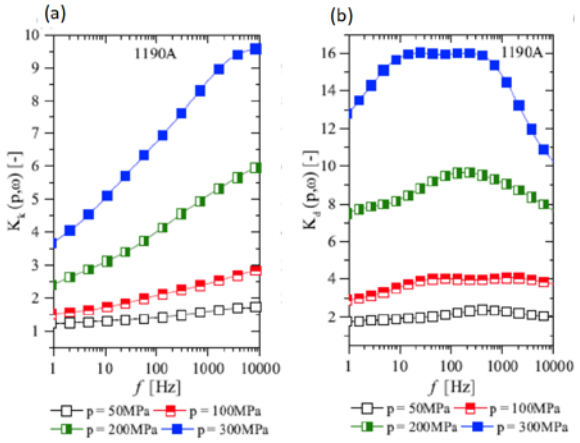

Figure 22: (a) $K_k(p,\omega)$ and (b) $K_d(p,\omega)$ of 1190A as functions of frequency for four selected pressures

From Fig. 22a one may observe that TPU 1190A stiffness is very sensitive to excitation frequency, particularly at highest pressure. At the same time excitation frequency has much smaller effect on material damping, Fig. 22b, and this is so for all pressures. One also observes that pressure has significant effect on both, stiffness and damping. At highest pressure stiffness increases for about 4 to 10 times, and its damping for about 10 to 16 times, depending on the frequency of excitation. It is also interesting to observe that at highest pressure damping start to decrease as soon as the excitation frequency is higher than 1000Hz.

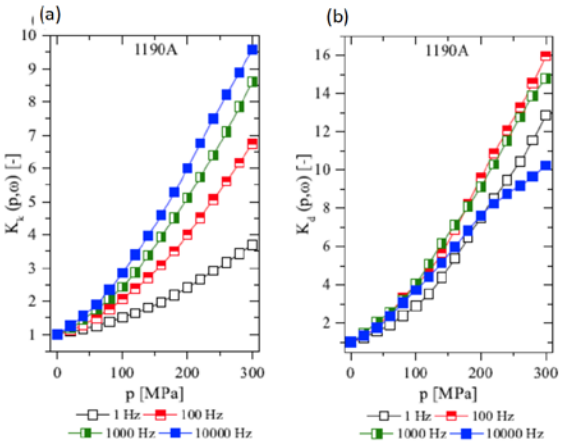

Figure 23: (a) $K_k(p,\omega)$ and (b) $K_d(p,\omega)$ of 1190A as functions of hydrostatic pressure at four selected frequencies

The effect of pressure is seen more clearly in Fig. 23, which shows $K_k(p,\omega)$ and $K(p,\omega)$ at four selected excitation frequencies, i.e., 1, 10, 1000 and 10000 Hz, as functions of pressure, within the range up to 300 MPa. The two figures, Figs. 22 and 23, essentially show the same information just presented in a different way. However, the different "angle of observation" provides quite different physical inside.

From Fig. 23b one sees that damping monotonically increases with applied hydrostatic pressure at all frequencies almost equally up to 200MPa when, for the highest excitation frequency, the slope of the increase declines. The improvement of damping relative to the damping at reference pressure, caused by hydrostatic pressure, is the largest at 100Hz excitation, followed by 1000Hz, 1Hz and 10000Hz.

Quite different is true for stiffness, displayed in Fig. 23a. Here one observes that stiffness monotonically increases with the applied hydrostatic pressure for all excitation frequencies, and the largest improvement is observed at the highest excitation frequency, and the smallest for the excitation of 1Hz. One also observes that the largest "gap" is observed between the excitation frequencies 1Hz and 100Hz.

All these observations confirm that the effect of pressure on stiffness and damping is nonlinear and need to be carefully investigated for each particular material to be used for the new generation damping elements. These observations also confirm that vibration isolation based on the patented *dissipative granular high-pressure technology* can surpass the existing solutions for several orders of magnitude and allows new generation engineering solutions in different areas of application.

5. Discussion on possible engineering applications

As mentioned in the introduction, in existing engineering solutions any improvement of material damping would "soften" the material, and any improvement of stiffens would either lead to bigger dimensions of a loaded body, or to lower damping of the used material. Any simultaneous improvement of damping and stiffness, as offered by the new *dissipative granular high-pressure technology*, would therefore have the potential for new engineering applications, which would not be achievable with the currently known technologies. We list a few examples to demonstrate the wide range of possible new applications:

- High-energy absorption in automotive industry where dampers are needed to reduce the peak forces under impact loading or reduce vibrations caused by non-harmonic excitations. Currently, any improvement of damping would lead to higher volume of the used damper. Newly developed dampers based on the high-pressure technology combine high energy absorption with high stiffness and therefore allow for small build-in volume. They exhibit

almost instantaneous response- and recovery time under vibrational and impact loading which is needed for safety applications.

- The use of the new dampers based on high pressure technology would substantially reduce vibrations, size and weight of currently used shock absorbers in the axels of vehicles. Particularly for heavy duty trucks the new dampers might replace currently used air suspensions.
- Passive car bumpers based on new technology will absorb more energy under impact loading and might be used for safety reasons in autonomous driving cars when getting out of control.
- Damper applications in foundations for heavy machines and railroads. The unique combination of high damping and high stiffness of the new dampers allows for applications where heavy loads or forces must be transferred into a fundament, yet high shock absorbance and vibration damping is needed. Such applications are the foundlings of heavy forge hummers or heavy sheet steel presses where repeating impact occurs.
- For high speed trains or high-speed freight trains high forces must be supported while vibrations must be minimized by rail carrying sleeper (ref patent). Heavy loads can be sustained by hydrostatically loaded polymers.
- Application of dampers for earthquake protection. As can be seen from the failure envelope of pressurized polymers, uniaxial- or two-dimensional pressure loading will cause shear failure of polymers, whereas three-dimensional pressure will be sustained up to extremely high loads. The reason that polymers can sustain almost infinitely high pressure allows their application for the protection of high-rise buildings, towers and bridges against s-waves emitted by earthquakes.

It must be stated however, that the proper selection of the size and geometry of the damper device, the choice of the proper polymeric material and the choice of the applied hydrostatic preloading of the damping element still remains to the skill and responsibility of the design engineer.

References

1. Emri I, Bernstorff B (2016). Dissipative bulk and granular systems technology, München: Europäisches Patentamt: EP2700839.
2. Emri I, Bernstorff B, Brehmer F, Kalamar A, Bek M, Oblak P (2014) Sleeper with damping element based on dissipative bulk or granular technology, München: Europäisches Patentamt, EP2700838.
3. Tschoegl NW (1989), The Phenomenological Theory of Linear Viscoelastic Behavior: An Introduction, Springer, New York
4. Knauss W G, Emri I, Lu H (2008) Mechanics of polymers: Viscoelasticity. In: Sarpe Jr., William N (ed) Springer handbook of experimental solid mechanics, 1st ed. Springer, New York: 49-95.
5. Deng T H, Knauss W G (1997) The temperature and frequency dependence of the bulk compliance of poly(vinyl acetate): A re-examination. J Mech. Of Time-Dep. Mat., 1:33-49
6. Tschoegl NW, Knauss WG, Emri I (2002), The effect of temperature and pressure on the mechanical properties of thermo- and/or piezorheologically simple polymeric materials in thermodynamic equilibrium: a critical review; Mechanics of time-dependent materials, 6:53-99
7. Tschoegl NW, Knauss WG, Emri I (2002) Poisson's ratio in linear viscoelasticity – a critical review. J Mech. Of Time-Dep. Mat., 6:3-51
8. Williams ML, Landel RF, Ferry JD (1955) 'The temperature dependence of relaxation mechanisms in amorphous polymers and other glass-forming liquids', J. Amer. Chem. Soc. 77, 3701–3707.
9. Emri I, von Bernstorff BS, Cvelbar R, and Nikonov AV (2005), Re-examination of the approximate methods for interconversion between frequency- and time-dependent material functions. Journal of Non-Newtonian Fluid Mechanics 129 (2), 75-84
10. Gergesova M, Zupančič B, Saprunov I, Emri I (2011), The closed form t-T-P shifting (CFS) algorithm. Journal of Rheology 55: 1-16
11. Martin M C (1986) Elements of thermodynamics, Prentice-Hall, Englewood Cliffs
12. Moonan WK, Tschoegl NW (1985). The effect of pressure on the mechanical properties of polymers. IV. Measurements in torsion. Journal of Polymer Science: Polymer Physics Edition, 23(4), 623–651.

13. Knauss WG, Emri I (1981). Non-linear viscoelasticity based on free volume consideration. Computers & Structures 23 (1-3): 123-128
14. Kralj A, Prodan T, and Emri I (2001). An apparatus for measuring the effect of pressure on the time-dependent properties of polymers, Journal of Rheology, 45 (4): 929-943
15. Emri I and Prodan T (2006). A measuring system for bulk and shear characterization of polymers, Experimental Mechanics 46: 429-439
16. Bregant D, Emri I (2013). Development and construction of the measuring device for analysing micro powders flowability, Diploma Thesis, University of Ljubljana, Faculty of Mechanical Engineering.
17. Bek M, Gonzalez-Gutierrez J, Lopez JAM, Bregant D, Emri I (2016). Apparatus for measuring friction inside granular materials - Granular friction analyzer, Powder Technol. 288 (2016) 255–265.
18. Venkatesh R, Voloshin A, Emri I, Brojan M, Govekar E (2019). Digital Image Correlation Based Internal Friction Characterization in Granular Materials, Exp. Mech. Experimental Mechanics, https://doi.org/10.1007/s11340-019-00570-8 already published
19. Bek M, Betjes J, Bernstorff B, and Emri I (2017). Viscoelasticity of new generation thermoplastic polyurethane vibration isolators. Phys. Fluids, vol. 29, no. 12.